Heliyon 10 (2024) e27160

Contents lists available at ScienceDirect

Heliyon

journal homepage: www.cell.com/heliyon

Research article

Differences in collateral vessel formation after experimental retinal vein occlusion in spontaneously hypertensive rats and wild-type rats

Masatoshi Omi *, Haruhiko Yamada, Hajime Takahashi, Hidetsugu Mori, Shimpei Oba, Yuki Hattori, Kaito Yokota, Keiko Toyama, Kanji Takahashi

Department of Ophthalmology, Kansai Medical University, Hirakata, Japan

ARTICLE INFO

Keywords:
Retinal vein occlusion
Collateral vessels
Hypertension
Animal model
Optical coherence tomography angiography
Sphingosine 1-phosphate receptor 1
Endothelial nitric oxide synthase

ABSTRACT

Objective: Retinal vein occlusion (RVO) can lead to visual impairment, but the development of collateral vessels can sometimes mitigate significant damage. This study aimed to investigate the relationship between collateral vessels and hypertension, the most common underlying condition associated with RVO, by comparing spontaneously hypertensive rats (SHRs) and wild-type Wister rats (WWRs). We also examined the differences between WWRs and SHRs in terms of sphingosine 1-phosphate receptor 1 (S1PR1) expression and its product nitric oxide synthase 3 (NOS3) expression, which are involved in the formation of collateral vessels after vascular occlusion.

Methods: Laser photocoagulation (PC) was used to occlude one randomly selected retinal vein in WWRs and SHRs, and the area surrounding the occluded vessel was examined using optical coherence tomography angiography. If reperfusion of the occluded vessel occurred within 2 weeks, the vessel was re-occluded repeatedly by PC. The number of eyes with successfully occluded vessels accompanied by collateral vessels was recorded. Then, WWRs and SHRs were divided into the following four groups: 1) control (no treatment), 2) vehicle (20% DMSO), 3) S1PR1 agonist (2 mg/mL SEW2871), and 4) S1PR1 antagonist (0.25 mg/mL VPC 23019) groups. The drugs were administered intravitreally in all groups except the control. The number of laser shots required for successful RVO was recorded. Histological evaluation and quantitative real-time PCR of S1PR1 and NOS3 were performed to elucidate the mechanisms underlying collateral vessel formation.

Results: The proportion of eyes achieving successful vein occlusion was lower in SHRs (4/12 eyes, 33.3%) than in WWRs (8/10 eyes, 80%, $p = 0.043$). NOS3 expression at 6 h after PC was significantly higher in WWRs than in SHRs ($p = 0.021$). In WWRs treated with SEW2871, vein occlusion failed in 7 of 10 eyes (70%). The expression of NOS3 was significantly higher in the SEW2871 treatment group than in the untreated group ($p < 0.001$). Furthermore, NOS3 expression was significantly higher after SEW2871 treatment in WWRs than in SHRs ($p = 0.011$).

Conclusion: In hypertensive environments, collateral vessels are less likely to develop, and S1PR1 may be involved in this phenomenon.

* Corresponding author.
E-mail address: omimasatoshi@gmail.com (M. Omi).

https://doi.org/10.1016/j.heliyon.2024.e27160
Received 8 November 2023; Received in revised form 16 February 2024; Accepted 26 February 2024
Available online 1 March 2024

1. Background/Introduction

Retinal vein occlusion (RVO) commonly affects middle-aged and/or older individuals with hypertension and can lead to significant vision impairment due to complications such as macular edema and neovascular glaucoma [1]. However, in some cases, the development of collateral vessels following RVO can improve the ischemic pathology and reduce severe complications [2]. Our previous study [3] using a mouse model of RVO and optical coherence tomography angiography (OCTA) demonstrated that occlusion of one retinal vein in the mice led to formation of collateral vessels in the deep layer of the retina. In that study, we confirmed that sphingosine 1-phosphate receptor 1 (S1PR1) and shear stress play significant roles in collateral vessel formation. However, it is important to acknowledge that young mice without underlying diseases, which may not fully reflect the actual clinical course of RVO, were utilized in that study. Therefore, in this study, we investigated the relationship between hypertension and collateral vessel formation using a common hypertensive animal model, the spontaneously hypertensive rat (SHR). The SHR, obtained via selective breeding of hypertensive Wistar rats, is a well-established animal model used to investigate hypertensive disease [4]. Retinal vessels in SHRs have a narrower diameter and reduced elasticity compared with those in normal rats [5,6]. There is limited research on RVO using SHRs [7], and there are no reports of laser-induced RVO in SHRs. The objective of our study was to investigate differences in vascular structural changes following RVO between SHRs and wild-type Wistar rats (WWRs) to explore the relationship between hypertension and collateral vessel formation. Furthermore, it has been reported that vascular shear stress activates S1PR1 in vascular endothelial cells, leading to the generation of nitric oxide (NO) via nitric oxide synthase 3 (NOS3) and resulting in vasodilation [8–10]. Therefore, we also investigated differences in S1PR1 expression and NOS3 expression between SHRs and WWRs.

2. Materials and methods

2.1. Animals

WWRs and SHRs were purchased from SLC Japan (Tokyo, Japan). All rats were housed in pathogen-free plastic cages under a 12/12-h light/dark cycle with free access to water and food (CA-1; CLEA Japan, Inc., Tokyo, Japan). All cages, water, bedding, and food were sterilized before use. For all experimental procedures, anesthesia was induced by intraperitoneal injection of 0.375 mg/kg medetomidine (Nippon Zenyaku Kogyo Co., Fukushima, Japan), 2.5 mg/kg butorphanol (Meiji Animal Health Co., Kumamoto, Japan), and 2.0 mg/kg midazolam (Sandoz K.K., Tokyo, Japan). The pupils were dilated using topical 0.5% tropicamide and 0.5% phenylephrine (Santen Pharmaceutical, Osaka, Japan).

2.2. Blood pressure measurements

The blood pressure of each rat was measured using the BP-98AL device (Softron Co., Tokyo, Japan), following the manufacturer's protocol. The rats were placed in a net holder equipped with a temperature controller set to 37 °C, and caudal arterial pressure was measured using an oscillometric cuff connected to the apparatus positioned at the base of the tail. Measurements were performed three times, and the average systolic blood pressure was recorded as the blood pressure of each rat.

2.3. Generation of RVO

Under deep anesthesia, WWRs and SHRs were injected intraperitoneally with 0.2 mL phosphate-buffer saline (PBS) containing 50 mg/mL Rose Bengal dye (Nacalai-Tesque, Kyoto, Japan). Within approximately 3 min after dye injection, laser photocoagulation (PC) was performed on the left eye of each rat using the GYC-2000 half-wavelength YAG laser with a wavelength of 532 nm (NIDEK Co, Gamagori, Japan) attached to a slit-lamp delivery system (Carl Zeiss SL 130, Jena, Germany). A laser spot size of 100 μm, a pulse duration of 100 ms, and an incident power of 250 mW were utilized to target the vessel and induce blood flow cessation in the retinal vein. For laser-induced occlusion, a single vessel located 1–2 optic nerve diameters away from the optic nerve head was randomly selected and coagulated.

2.4. Vascular occlusion and reperfusion monitoring using optical coherence tomography angiography (OCTA)

Ten 8-week-old male WWRs and 12 age-matched SHRs were used in this experiment. After occluding a single retinal vein in the animals using PC, the area surrounding the occluded vessel was monitored over time using OCTA (RS-3000 Advance system, NIDEK Co.). The OCTA system had an optical resolution of 20 μm in the XY direction and 7 μm in the Z direction. Vessel observations using OCTA were conducted on days 2, 4, 7, 9, 11, 14, 16, 18, and 21 after PC. On observation days 2, 4, 7, 9, 11, and 14, if the occluded vein showed reperfusion, additional PC was performed immediately to re-occlude the same vessel. This procedure was repeated until day 14 of the observation period. On days 16, 18, and 21, only observations were conducted. If the blood flow of the coagulated vessels remained blocked for more than 1 week, it was judged as successful occlusion. The number of eyes with a successfully occluded vessel was recorded and measured.

2.5. S1PR1 agonist and antagonist administration

We evaluated 33 newly prepared eyes from 8-week-old male WWRs and 32 eyes from age-matched SHRs under the same

conditions. The WWRs and SHRs were each divided into four groups: control rats receiving no drug administration, rats treated with vehicle (dimethyl sulfoxide [DMSO]) only, rats treated with the S1PR1 agonist SEW2871 (SEW, Cayman Chemical, Ann Arbor, MI, USA), and rats treated with the S1PR1 antagonist VPC23019 (VPC, Cayman Chemical). Solutions of 2 mg/mL SEW and 0.25 mg/mL VPC were prepared by dissolving each drug in 100% DMSO and diluting with 50% Tween 20 prior to administration; the final concentration of DMSO was 20%. The SEW and VPC concentrations used in the study were determined based on the manufacturer's recommendations. Each rat was administered 2 μL of the respective drug solution through the pars plana using a microinjector (Narishige, Tokyo, Japan). At 6 h after injection, we attempted to occlude a single retinal vein in each injected eye using PC, as described above. The number of PC shots required to achieve complete occlusion was recorded. The eyes with vessels that could not be occluded after a maximum of 200 PC shots were considered "not occluded".

2.6. Quantitative real-time PCR (qRT-PCR)

In WWRs and SHRs, NOS3 and S1PR1 expression was assessed by qRT-PCR at 6 h after PC occlusion of one vein and at 6 h after administration of each drug (DMSO, SEW2871, and VPC23109). Fresh rats that had not been used previously were used for this experiment. mRNA from the entire retina of age-matched rats without PC or drug administration served as controls. All rats were euthanized by cervical dislocation after deep anesthesia. Immediately after isolating whole retinas from each eye, the retinas were stored in RNA later® solution (Thermo Fisher Scientific, Waltham, MA, USA) to prevent degradation. The isolated retinas were then homogenized using the Biomasher tissue grinder (Nippi Inc., Tokyo, Japan). Total RNA was isolated using the RNeasy Plus Mini® Kit (Qiagen, Venlo, The Netherlands) according to the manufacturer's protocol. The total RNA was reverse transcribed to generate cDNA using the SuperScript® VILO™ cDNA Synthesis Kit (Thermo Fisher Scientific). The reverse-transcribed cDNA was subsequently subjected to qRT-PCR using the Thermal Cycler Dice® Real Time System II (TAKARA Bio, Otsu, Shiga, Japan). All reactions were prepared as a total volume of 25 μL using the SYBR® Premix Ex *Taq*II™ PCR Kit (TAKARA Bio) following the manufacturer's protocol. The target sequences used in this study were amplified using the following primer sequences: Gapdh, (forward) 5′-GGCACAGTCAAGGCTGAGAATG-3′ and (reverse) 5′-ATGGTGGTGAAGACGCCAGTA-3′; S1PR1, (forward) 5′-ACTACACAACGGCAGCAACAG-3′ and (reverse) 5′-GATGGAAAGCAGGAGCAGAG-3′; and NOS3 (forward) 5′-CAAGACCGATTACACGACATTGAGA-3′ and (reverse) 5′-TGAGGACTTGTCCAAACACTCCAC-3′.

The mRNA expression levels of the target genes in each group were normalized to those of Gapdh, used as the internal control, and were calculated using the standard curve method.

2.7. Immunohistochemical staining of retinal flat mounts

Fresh rats that had not been used previously were used for this experiment. In WWRs and SHRs, one retinal vein was occluded with PC. Six hours later, deeply anesthetized rats were sacrificed by intracardial perfusion with fluorescein isothiocyanate-labeled dextran (FITC/dextran) (Sigma-Aldrich, St. Louis, USA) adjusted to 0.5% in PBS after thoracotomy. Following FITC/dextran perfusion, the eyes were enucleated and fixed in 4% paraformaldehyde for 10 min. The anterior portion of the eyeball was then dissected, and the posterior portion was fixed again in 4% paraformaldehyde for 50 min. Whole retinas were isolated and permeabilized in PBS containing 4% Block Ace blocking reagent (DS Pharma Biomedical, Osaka, Japan) and 0.5% Triton X-100 for 3 h at room temperature.

For whole-mount immunolabeling of the retinas, we used an anti-S1PR1 monoclonal antibody (human anti-mouse S1PR1, 1:100; Santa Cruz Biotechnology, Santa Cruz, CA, USA) and Alexa Fluor-647 secondary antibody (1:200) to detect S1PR1. The isolated retinas were incubated in the primary antibody solution at 4 °C for 24 h with shaking. After several washes in PBS, the retinas were incubated for 4 h at room temperature in the secondary antibody solution.

To perform flat mount preparations, several cuts were made from the edge of the retina towards the center after thoroughly washing the retina in PBS several times. The retinas were then flattened and mounted using ProLong Gold antifade reagent (Life Technologies, Eugene, OR, USA) and cover-slipped. Tissue samples were observed using a confocal laser microscope (FV3000, Olympus Co, Tokyo, Japan).

A negative control was prepared by omitting the primary antibody from the immunostaining process and performing all other steps as above.

2.8. Statistical analysis

The percentages of eyes with successful vein occlusion were compared using Fisher's exact test. The mRNA expression levels of NOS3 and S1PR1 in whole retinas, quantified by qRT-PCR, were compared using ANOVA and the Tukey–Kramer post-hoc test. All statistical tests were performed and analyzed using JMP software (SAS Institute Inc., Cary, NC, USA). $p < 0.05$ was considered to indicate statistical significance. Prior to performing the statistical analyses, the normality of the data was confirmed using the normal probability plot, Shapiro–Wilk test, and O'Brien test. All values are presented as means unless stated otherwise.

2.9. Ethics statement

All animal experiments followed the guidelines of the Association for Research in Vision and Ophthalmology Statement for the Use of Animals in Ophthalmic and Vision Research and were approved by Kansai Medical University (approval number: A2020-67).

3. Results

3.1. Systolic blood pressure in WWRs and SHRs

Blood pressure was significantly higher by 31.2% in 8-week-old SHRs (n = 12, 177.3 ± 16.2 mmHg) than in 8-week-old WWRs (n = 10, 135.1 ± 12.1 mmHg, $p < 0.001$).

3.2. Rate of successful vein occlusion in WWRs and SHRs

The rates of successful collateral vessel development and maintenance of vein occlusion resulting from repeated PC were evaluated in both WWRs and SHRs. The rate of successful occlusion was 33% (4/12 eyes) in SHRs versus 80% (8/10 eyes) in WWRs, with a significantly 2.4-fold higher rate in the WWRs than SHRs ($p = 0.043$). Representative examples from both groups are shown in Fig. 1a and b. For all rats, Table 1 shows the time points at which reperfusion was observed by OCTA and PC was performed.

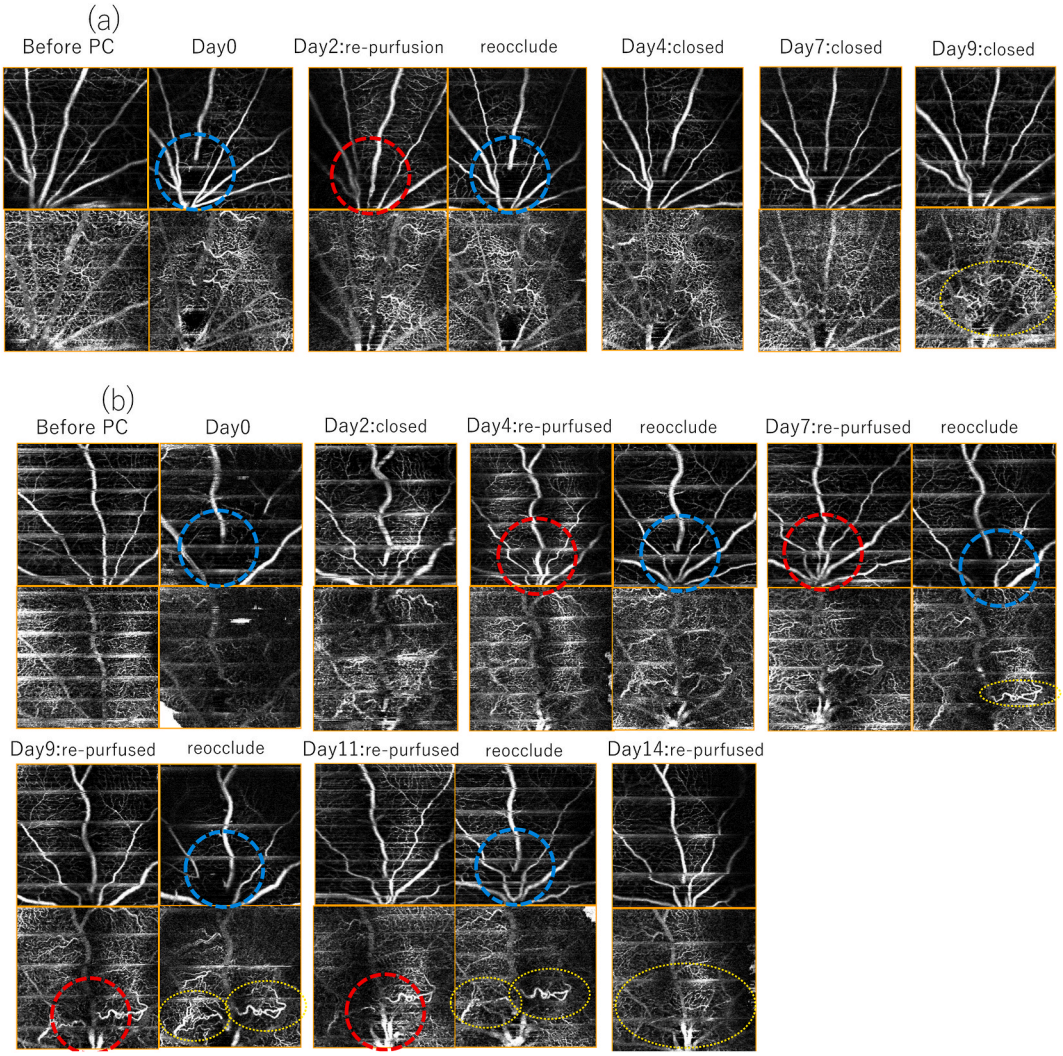

Fig. 1. Exemplary optical coherence tomography angiography (OCTA) images of experimental retinal vein occlusion (RVO) in Wild-type Wister rats (WWRs) and spontaneously hypertensive rats (SHRs). a) Exemplary OCTA image of experimental RVO in WWRs. On day 0, the vein of the rat was occluded using photocoagulation (PC), as indicated by the blue dotted circle. On day 2, reperfusion of the occluded vessel occurred, as shown by the red dotted circle. Subsequently, the vein was re-occluded using PC (blue dotted circle). The occlusion was maintained for over a week (successful occlusion), and the formation of collateral vessels can be observed inside the yellow dotted circle. b) Exemplary OCTA image of experimental RVO in SHRs. On day 0, the vein of the rat was occluded using PC, indicated by the blue dotted circle. On day 4, reperfusion of the occluded vessel was observed (red dotted circle), leading to the vein being re-occluded (blue circle). On days 4, 7, 9, and 11, the vein experienced repeated reperfusion and required additional PC (occlusion failure). Notably, the collateral vessel that appeared until day 11 disappeared by day 14 (yellow dotted circle).

Table 1
Timing of treatment and final judgments in all rats.

Rat	Day2	Day4	Day7	Day9	Day11	Day14	Day16	Day18	Day21	judgement
WWR1	R	O	O	O	O	O	O	O	O	successfully occlusion
WWR2	R	O	R	O	R	O	O	O	O	successfully occlusion
WWR3	O	O	O	O	O	O	O	O	O	successfully occlusion
WWR4	R	R	R	R	R	O	O	O	O	successfully occlusion
WWR5	R	O	O	O	O	O	O	O	O	successfully occlusion
WWR6	R	O	O	O	O	O	O	O	O	successfully occlusion
WWR7	O	R	R	O	O	O	O	O	O	successfully occlusion
WWR8	O	O	O	O	O	O	O	O	O	successfully occlusion
WWR9	R	R	R	R	R	R	R	R	R	occlusion failure
WWR10	R	R	R	R	R	R	R	R	R	occlusion failure
SHR1	O	R	R	R	R	R	R	R	R	occlusion failure
SHR2	R	R	R	R	R	R	R	R	R	occlusion failure
SHR3	O	R	R	O	R	R	R	R	R	occlusion failure
SHR4	O	O	R	R	R	R	R	R	R	occlusion failure
SHR5	R	R	R	R	R	R	R	R	R	occlusion failure
SHR6	O	R	R	R	R	R	R	R	R	occlusion failure
SHR7	R	R	R	R	R	R	R	R	R	occlusion failure
SHR8	R	R	R	R	R	R	R	R	R	occlusion failure
SHR9	R	R	O	O	O	O	O	O	O	successfully occlusion
SHR10	R	R	R	R	R	O	O	O	O	successfully occlusion
SHR11	R	O	O	O	O	O	O	O	O	successfully occlusion
SHR12	R	O	O	O	O	O	O	O	O	successfully occlusion

R: reperfusion, O: occluded WWR1 is the rat in Figua1 a) and SHR1 is the rat in Figua1 b).

One retinal vein was occluded by laser on Day 0. Vessel observations using OCTA were conducted on Days 2, 4, 7, 9, 11, 14, 16, 18, and 21 after PC. On observation Days 2, 4, 7, 9, 11, and 14, if the occluded vein showed reperfusion, additional PC was performed immediately to re-occlude the same vessel. This procedure was repeated until Day 14 of the observation period. On Days 16, 18, and 21, only observations were conducted. If the blood flow of the coagulated vessels remained blocked for more than 1 week, it was judged as successful occlusion.

3.3. Immunofluorescence imaging in retinal flat mounts

To visualize the expression of S1PR1 in the retinas of RVO model rats, we conducted immunohistochemical staining of S1PR1 using retinal flat mounts perfused with FITC/dextran (Fig. 2a, b, 2c). In both the WWRs and SHRs, we observed strong expression of S1PR1 in the periphery of the occluded retinal veins. (Fig. 2a and b). On the other hand, no S1PR1 expression was observed in vessels without vein occlusion. (Fig. 2a and b).

3.4. qRT-PCR of NOS3 in whole retinas after vein occlusion in WWRs and SHRs

NOS3 expression was significantly higher after than before PC in both WWRs (2.4 fold, $p < 0.001$) and SHRs (2.2 fold, $p < 0.001$, Fig. 3a). Additionally, when comparing NOS3 expression at 6 h after PC between WWRs and SHRs, NOS3 expression was higher in WWRs than SHRs (1.3 fold, $p = 0.021$, Fig. 3a).

3.5. Effects of the S1PR1 agonist and antagonist on the RVO success rate after intravitreal injection

RVO was observed in all eyes of the control, DMSO-treated, and VPC-treated groups of WWRs and in the control, DMSO-treated, SEW-treated, and VPC-treated groups of SHRs. However, in the SEW-treated WWRs, 7 of 10 eyes did not experience RVO even after administration of over 200 PC shots, which was a significantly higher number than those in the other groups ($p < 0.001$, Table 2).

The three eyes with successful occlusion in the SEW-treated WWRs required significantly more laser shots for vein occlusion compared with any of the other groups ($p < 0.001$, Fig. 3b). In the SHRs, significantly more laser shots were needed for vein occlusion in the SEW-treated than control group (6.6 fold, $p < 0.001$, Fig. 3b). Furthermore, significantly more PC shots were required in the SEW-treated group than VPC-treated group (1.6 fold, $p = 0.049$, Fig. 3b).

3.6. S1PR1 and NOS3 expression according to qRT-PCR after treatment with the S1PR1 agonist and antagonist

There was no significant difference in S1PR1 expression between before and after treatment with DMSO, SEW or VPC ($p > 0.05$). In contrast, the expression of NOS3 was significantly increased after each drug treatment compared with the control groups ($p < 0.001$, Fig. 3c). Furthermore, the expression of NOS3 after SEW treatment was significantly higher in the WWRs than SHRs (1.4 fold, $p = 0.011$, Fig. 3c).

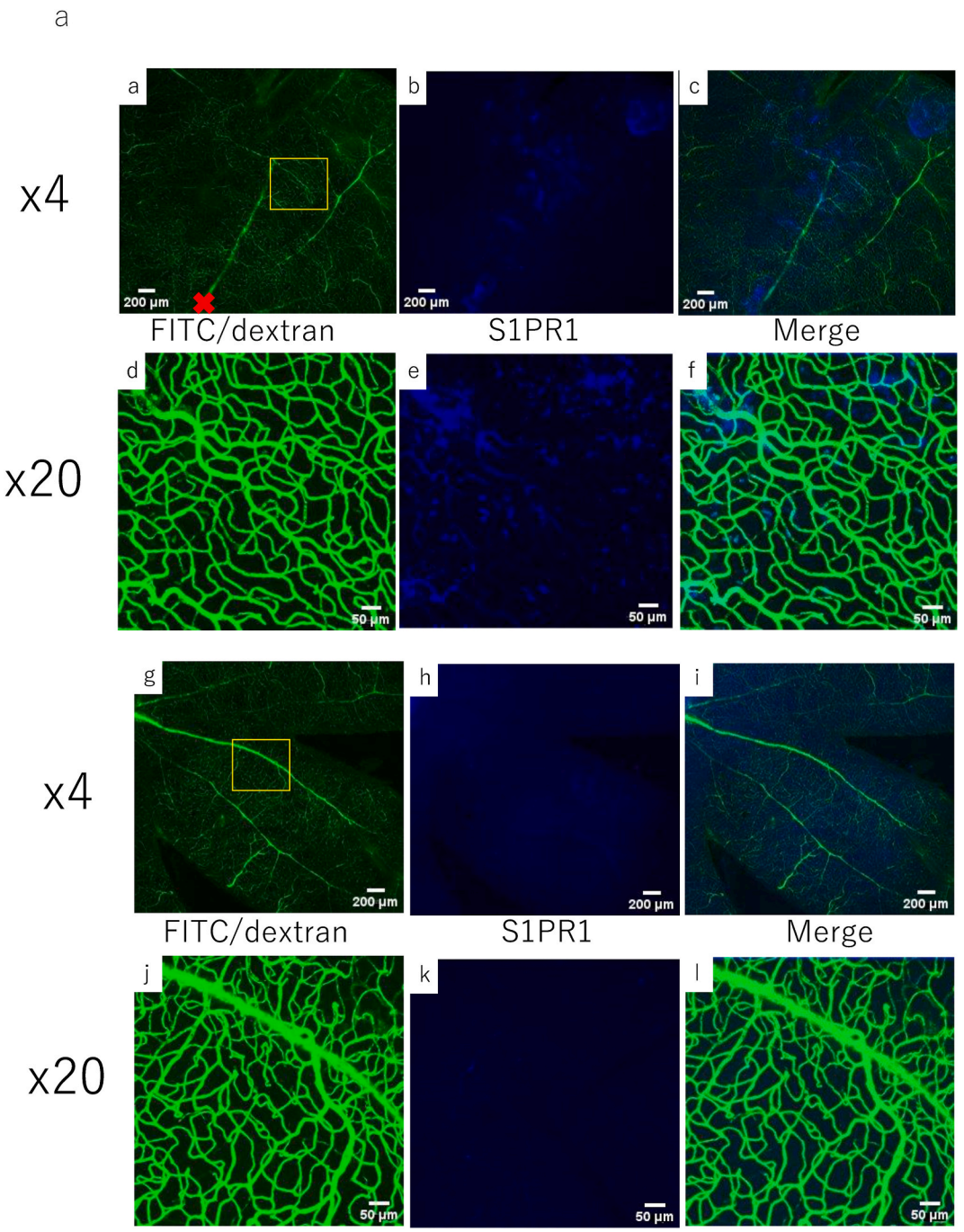

Fig. 2. a): Immunofluorescence imaging of retinal flat mounts in Wild-type Wister rats (WWRs): occluded area (a–f) and non-occluded area (g–l). a, g: fluorescein isothiocyanate - labeled dextran (FITC/dextran) perfused retinas at 6 h after photocoagulation (PC). The red X indicates the site of vein occlusion. b, h: Immunohistochemical staining of sphingosine 1-phosphate receptor 1 (S1PR1) at 6 h after PC. c, I: Merged image from a, g and b, h. d, j: Enlarged view inside the yellow rectangle seen in a, g. e, k: Enlarged image from b, h showing enhanced S1PR1 expression along the blood vessels. f, l: Merged image of those from d, j and e, k. In b, h, enhanced S1PR1 expression was detected along the retinal vein occlusion. In e, k, enhanced S1PR1 expression was detected along the blood vessels.
Fig. 2b): Immunofluorescence imaging of retinal flat mounts in spontaneously hypertensive rats (SHRs): occluded area (m–r) and non-occluded area (s–x): m, s: FITC/dextran-perfused retinas at 6 h after PC. The red X indicates the site of vein occlusion. n, t: Immunohistochemical staining of S1PR1 at 6 h after PC. O, u: Merged image of those from m, s and n, t. p, v: Enlarged view of the yellow rectangle seen in m, s. q, w: Enlarged image of that from n, t. r, x: Merged image of those from p, v and q, w. In n, t, enhanced S1PR1 expression was detected along the retinal vein occlusion. In q, w, enhanced S1PR1 expression was detected along the blood vessels.
Fig. 2c): Immunofluorescence imaging of retinal flat mounts in WWRs as a negative control (NC):in the occluded (NC1–NC6) and non-occluded

(NC7–NC12) areas: NC1, NC7: FITC/dextran-perfused retinas at 6 h after PC. The red X indicates the site of vein occlusion. NC2, NC8: Immunohistochemical staining of S1PR1 at 6 h after PC. NC3, NC9: Merged image of the images from NC1, NC7 and NC2, NC8. NC4, NC10: Enlarged view of the yellow rectangle in NC1, NC7.NC5, NC11: Enlarged image from NC2, NC8 showing enhanced S1PR1 expression along the blood vessels. NC6, NC12: Merged image of the image from NC4, NC10 and NC5, NC11.

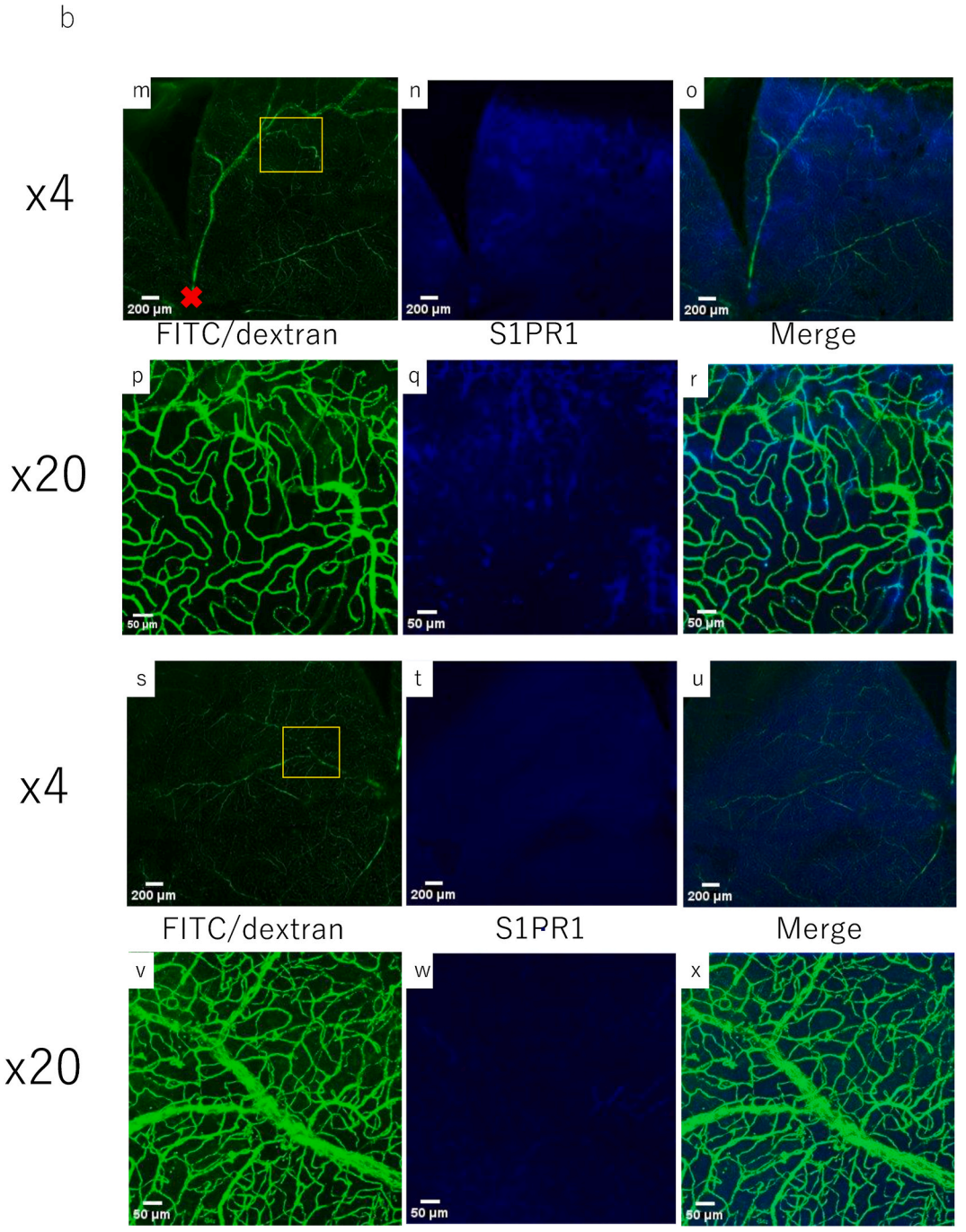

Fig. 2. (*continued*).

4. Discussion

In clinical practice, RVO occurs predominantly in middle-aged and/or older adults with hypertension as an underlying condition. However, experimental studies using hypertensive animal models to investigate the mechanisms of RVO are lacking. The aim of this study was to induce experimental RVO in SHRs to gain a better understanding of the pathogenesis of RVO. We performed OCTA along

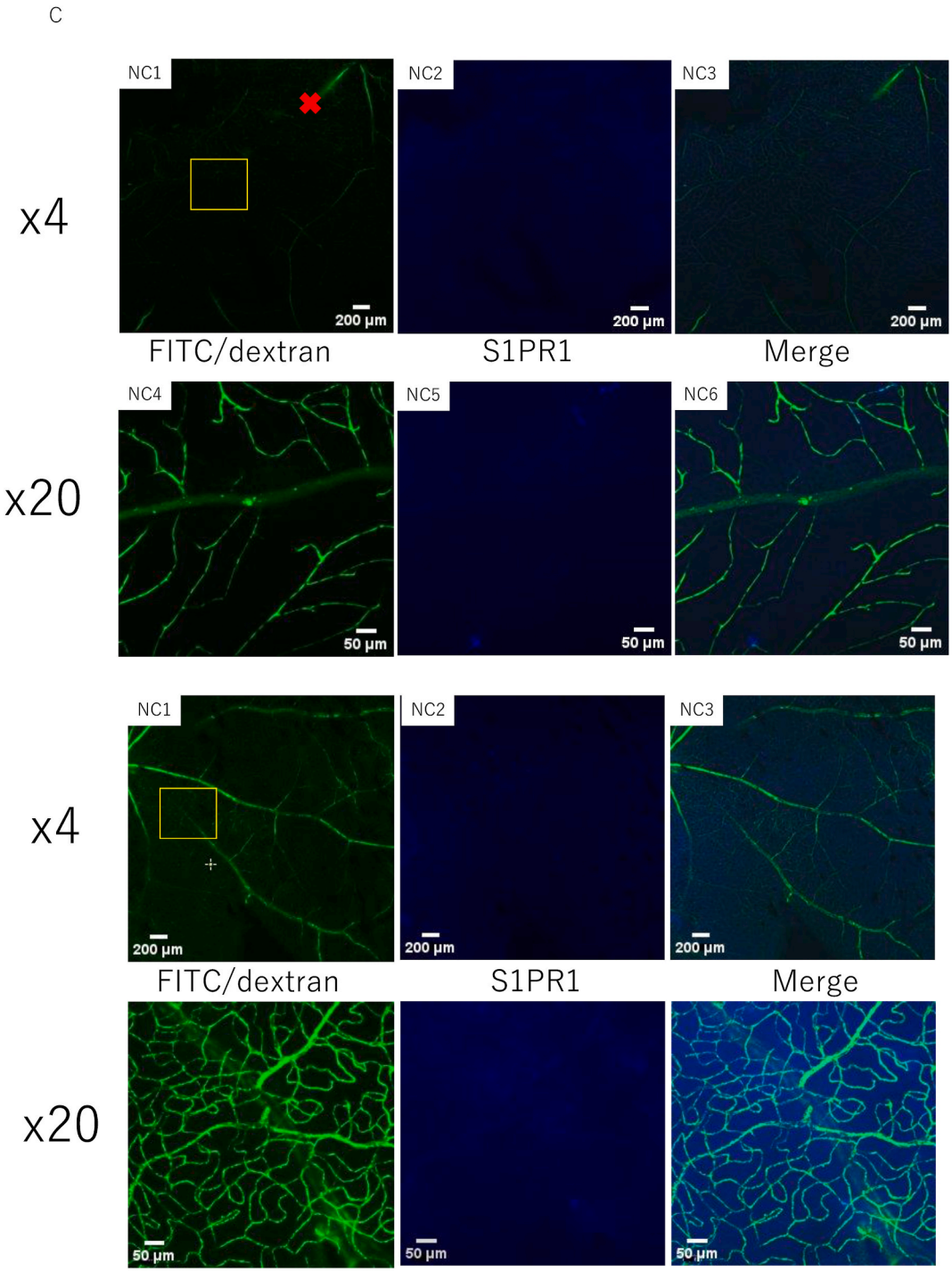

Fig. 2. (*continued*).

with histological evaluations to examine the formation of collateral vessels and identify the differences between SHRs and normal rats.

Several studies in the fields of cardiology and neurosurgery have explored ischemic injury and collateral vessel formation by occluding arteries in WWRs and SHRs [11–13]. Those studies consistently reported that SHRs exhibit reduced collateral vessel formation and increased ischemic damage compared with WWRs. Li et al. demonstrated that existing pial collateral vessels on the brain surface exhibited impaired elasticity and reduced sensitivity to shear stress in SHRs compared with WWRs [14]. Until now, most of the vascular occlusion models using SHRs have focused on arterial occlusion, and there is no such model for vein occlusion. Additionally, previous laser-induced RVO models did not utilize SHRs. As a result, we decided to develop a laser-induced RVO model using SHRs. By

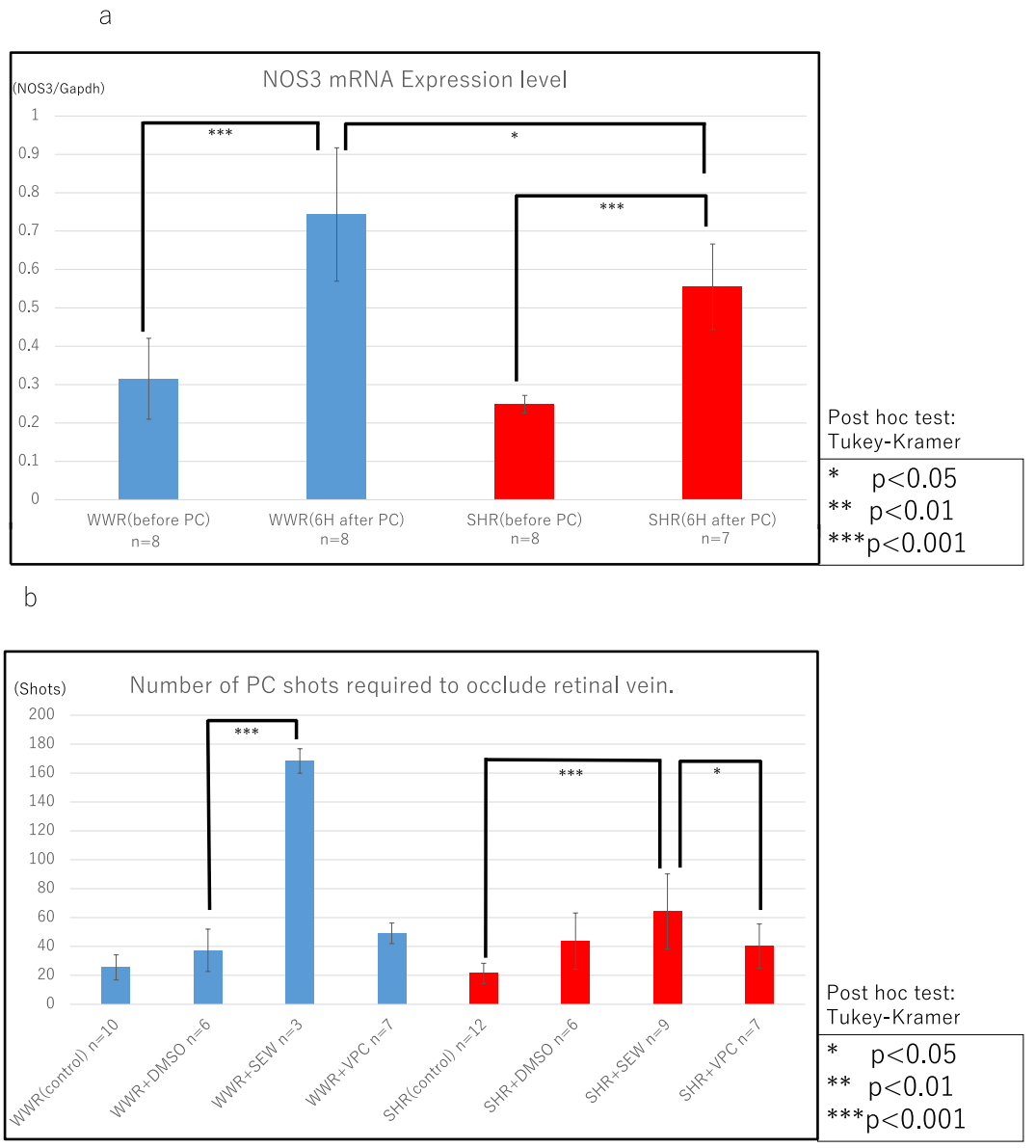

Fig. 3. a): nitric oxide synthase 3 (NOS3) expression quantified by qRT-PCR in the whole retina of Wild-type Wister rats (WWRs) and spontaneously hypertensive rats (SHRs) before photocoagulation (PC) and 6 h after PC. The Y-axis indicate these are relative NOS3/gapdh to untreated control retina values. In both WWRs and SHRs, the expression of NOS3 was significantly higher at 6 h after PC than before PC ($p < 0.001$, Tukey–Kramer post-hoc test). Before the PC procedure, there was no significant difference in NOS3 expression between WWRs and SHRs. However, at 6 h after PC, NOS3 expression was predominantly higher in WWRs than SHRs (1.3 fold, $p = 0.02$, Tukey–Kramer post-hoc test).
Fig. 3b): The number of PC shots required for vein occlusion before and after each drug administration. The WWRs and SHRs were each divided into four groups: control rats receiving no drug administration, rats treated with vehicle (dimethyl sulfoxide [DMSO]), rats treated with the S1PR1 agonist SEW2871, and rats treated with the S1PR1 antagonist VPC23019. The number of PC shots required to achieve retinal vein occlusion was higher in the SEW-treated group than control group in both WWRs and SHRs ($p < 0.001$, Tukey–Kramer post-hoc test). Specifically, in the SEW-treated WWRs, the three eyes that could be occluded required significantly more laser shots compared with any of the other groups ($p < 0.001$, Tukey–Kramer post-hoc test). In SHRs, a significantly greater number of PC shots was required after SEW than VPC treatment (1.5 fold, $p < 0.05$, Tukey–Kramer post-hoc test).
Fig. 3c): NOS3 expression in all retinas of WWRs and SHRs before and after administration of each drug. The Y-axis indicate these are relative NOS3/gapdh to untreated control retina values. The expression of NOS3 was significantly increased in dimethyl sulfoxide (DMSO), SEW, and VPC -treated groups compared with the pre-treatment (control) group ($p < 0.001$, Tukey–Kramer post-hoc test). When comparing the expression of NOS3 between the SEW-treated WWRs and SHRs, the expression of NOS3 was significantly higher in the former (1.4 fold, $p < 0.01$, Tukey–Kramer post-hoc test).

C

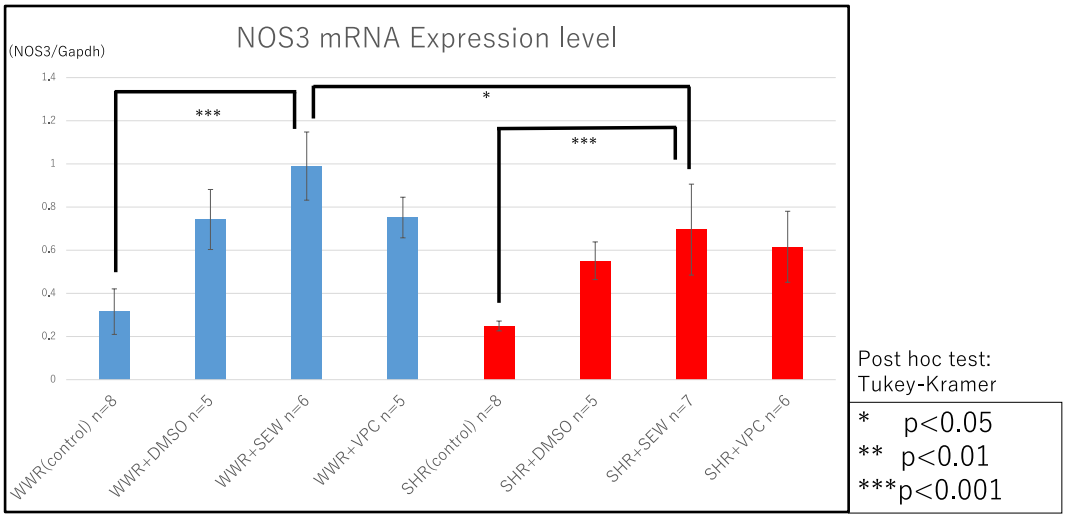

Fig. 3. (*continued*).

Table 2
The number of eyes that were not occluded after PC accompanied by intravitreal injection.

	Control group	DMSO group	SEW group	VPC group
WWR	0 eyes/10 eyes (0%)	0 eyes/6 eyes (0%)	7 eyes/10 eyes (70%)	0 eyes/7 eyes (0%)
SHR	0 eyes/12 eyes (0%)	0 eyes/6 eyes (0%)	0 eyes/9 eyes (0%)	0 eyes/7 eyes (0%)

The number of eyes that were not occluded was significantly greater in WWRs treated with SEW than in the other groups ($p < 0.001$).

conducting OCTA and molecular and histological evaluations, we aim to identify potential differences in collateral vessel formation under RVO.

In this study, we created a rat model of RVO by occluding the retinal vein of each rat. In contrast to mice, single occlusion of a retinal vein in rats often leads to reperfusion within a few days [15,16]. This phenomenon requires repeated occlusions to achieve permanent vein occlusion. OCTA, which relies on blood flow reflection [17], enabled us to visualize regions without blood flow and to identify truly occluded areas that may not be visible by static imaging of blood vessels. In addition, unlike conventional angiography using contrast media, OCTA-based angiography is less invasive to the animal and allows for repeated procedures on the same animal. During the repeat vein occlusion process, we consistently observed formation of well-developed collateral vessels once the eyes achieved permanent vein occlusion. This observation led us to hypothesize that when collateral vessels are sufficiently developed, venous blood flow through the occluded vein is redirected to the non-occluded vessels, bypassing the occlusion site. To further investigate this hypothesis, we compared the percentage of eyes attaining successful occlusion between WWRs and SHRs. The number of successful occlusions was predominantly lower in SHRs than WWRs. Additionally, once occluded, the veins were more prone to reopening in SHRs than in WWRs.

To delve into the molecular mechanisms underlying these observations, we performed real-time PCR analysis. Although stimulation of S1PR1 ultimately leads to NO production, NO exists as a gas and is therefore difficult to capture. Therefore, we instead evaluated NOS3, the enzyme responsible for NO production. Real-time PCR demonstrated that NOS3 expression was predominantly lower in SHR than WWR retinas at 6 h after PC. NOS3, found in vascular endothelial cells, plays a role in vasodilation by producing NO [18], and activation of NOS3 has been implicated in collateral vessel formation [19]. Therefore, the lower expression of NOS3 in SHRs than in WWRs suggests that reduced expression of NOS3 is involved in the impaired formation of collateral vasculature in retinal vein occlusion.

Regarding the factor that contributed to regulation of NOS3 expression, previous research has highlighted shear stress as an activator of S1PR1, leading to production of NO via NOS3 [8–10]. To explore this further, we conducted immunostaining of S1PR1 in the retina at 6 h after retinal vein occlusion. In both WWRs and SHRs, we observed S1PR1 expression upstream of vessels that had undergone vein occlusion, but no S1PR1 expression was seen in vessels that had not undergone occlusion. This suggests that vein occlusion in rat retinal veins increases shear stress in the peripheral vessels of the eyes and enhances S1PR1 expression. Then, we examined the responsiveness of the retinal vasculature after vein occlusion to a S1PR1 agonist (SEW) and antagonist (VPC) in both WWRs and SHRs. After intravitreal injection of SEW and VPC in both rat types, we induced RVO. In the SHRs, a greater number of PC shots was required in the SEW-treated group than in the control group. However, in the SEW-treated WWRs, the retinal veins remained

un-occluded even after administering over 200 laser shots. Furthermore, when comparing the expression of NOS3 after SEW administration between WWRs and SHRs using real-time PCR, we observed predominantly lower NOS3 expression in the SHRs than WWRs. These findings suggest weaker expression of S1PR1 in SHRs than WWRs. Thus, S1PR1 may potentially influence the formation of collateral vessels. Taken together, these results suggest that alterations in S1PR1 activity play a role in the impairment of collateral vessel formation.

It is important to acknowledge the limitations of our study. First, the model of RVO we employed involved artificial occlusion induced by multiple cycles of PC, which may not fully mimic the pathophysiology of RVO in clinical practice. Clinical RVO often occurs due to thrombus formation under a background of atherosclerosis, introducing additional factors that are not simulated in our model [1]. This may limit the generalizability of our findings to the clinical setting. Furthermore, our study did not specifically account for the potential effects of PC itself and the inflammation induced by repeated PC. These factors could potentially influence the outcomes and interfere with the mechanisms underlying collateral vessel formation [20] and the response to S1PR1 modulation[21 22]. Second, we observed high expression of S1PR1 in the periphery of the occluded retinal veins. Some might argue that we should examine the localization of NO or NOS3, which are directly involved in vasodilation. However, direct visualization of NO can be challenging and NOS3 is readily destroyed during the fixation process. Furthermore, proving the relationship between shear stress and NOS3 via NOS3 localization might also be difficult. Therefore, we believe our hypothesis can be supported by monitoring the NOS3 trend using real-time PCR, without the need for immunostaining. Additionally, while we focused on S1PR1 as a shear stress-related factor, it is important to note that other factors are reportedly involved in shear stress responses, such as membrane-associated guanylate kinases, WW and PDZ domain containing 1 [21], and transient receptor potential vanilloid 4 [14,22]. We did not examine the activities of these factors, but their potential interactions with S1PR1 could provide a more comprehensive understanding of the mechanisms involved in collateral vessel formation. In addition, inflammation [23,24] and S1P [25] are involved in S1RP1 and NOS3 signaling other than that involved in shear stress, but these were not investigated in this study. To enhance our understanding of collateral vessel formation and the underlying factors, future studies should consider these limitations and aim to replicate the clinical scenario more accurately while investigating the interactions among various shear stress-related factors. By addressing these limitations, we can gain a better understanding of the complex mechanisms involved in collateral vessel formation and potentially identify new targets for therapeutic interventions in RVO.

This study has significant implications in the field of RVO research and has provided valuable insights into the impact of hypertension on the severity of RVO. The observation that both collateral vessel development and vessel obstruction were weaker in SHRs than WWRs suggests that hypertension may negatively influence the formation of collateral vessels. This could potentially contribute to the pathogenesis and progression of RVO in clinical practice. Moreover, this study demonstrated reduced sensitivity of S1PR1 in SHRs compared with WWRs, implying that impaired S1PR1 signaling may be a contributing factor to the decreased vascular elasticity observed in SHRs, which is consistent with previous research. Understanding the mechanisms underlying the reduced S1PR1 sensitivity and its impact on vascular responses can provide valuable insights into the pathophysiology of RVO and potentially guide the development of therapeutic interventions targeting S1PR1 signaling. However, further studies are necessary to fully elucidate the process of collateral vessel formation in RVO. Investigating the complex interplay among hypertension, S1PR1 signaling, and other factors involved in shear stress responses will be crucial for comprehensive understanding of the underlying mechanisms. Continued research in this area holds promise for the development of novel strategies for the prevention and treatment of RVO and its associated complications.

Data availability statement

Data will be made available on request.

CRediT authorship contribution statement

Masatoshi Omi: Writing – original draft, Visualization, Resources, Project administration, Methodology, Investigation, Funding acquisition, Formal analysis, Data curation, Conceptualization. **Haruhiko Yamada:** Writing – review & editing, Supervision, Project administration, Methodology, Investigation, Data curation, Conceptualization. **Hajime Takahashi:** Validation, Methodology, Conceptualization. **Hidetsugu Mori:** Validation, Supervision, Conceptualization. **Shimpei Oba:** Validation, Formal analysis, Data curation. **Yuki Hattori:** Validation, Formal analysis, Data curation. **Kaito Yokota:** Validation, Formal analysis, Data curation. **Keiko Toyama:** Validation, Resources, Formal analysis. **Kanji Takahashi:** Writing – review & editing, Supervision, Project administration.

Declaration of generative AI and AI-assisted technologies in the writing process

During the preparation of this work the author used Chat GPT3.5 in order to proofread English. After using this tool, the author reviewed and edited the content as needed and takes full responsibility for the content of the publication.

Declaration of competing interest

The authors declare the following financial interests/personal relationships which may be considered as potential competing interests:Masatoshi Omi reports financial support was provided by KAKENHI Grant in-Aid for Scientific Research C. Masatoshi Omi reports financial support was provided by Jhonson & Jhonson Surgical Vision. If there are other authors, they declare that they have no

known competing financial interests or personal relationships that could have appeared to influence the work reported in this paper.

Acknowledgements

We gratefully acknowledge the work of past and present members of our laboratory and medical office members.

References

[1] Risk factors for branch retinal vein occlusion. The eye disease case-control study group, Am. J. Ophthalmol. 116 (3) (1993) 286–296.
[2] N.L. Christoffersen, M. Larsen, Pathophysiology and hemodynamics of branch retinal vein occlusion, Ophthalmology 106 (11) (1999) 2054–2062, https://doi.org/10.1016/S0161-6420(99)90483-9.
[3] H. Takahashi, K. Nakagawa, H. Yamada, et al., Time course of collateral vessel formation after retinal vein occlusion visualized by OCTA and elucidation of factors in their formation, Heliyon 7 (1) (2021) e05902, https://doi.org/10.1016/j.heliyon.2021.e05902 [published Online First: 20210105].
[4] K. Okamoto, K. Aoki, Development of a strain of spontaneously hypertensive rats, Jpn. Circ. J. 27 (1963) 282–293, https://doi.org/10.1253/jcj.27.282.
[5] W. Leskova, R. Warar, N.R. Harris, Altered retinal hemodynamics and mean circulation time in spontaneously hypertensive rats, Invest. Ophthalmol. Vis. Sci. 61 (10) (2020) 12, https://doi.org/10.1167/iovs.61.10.12.
[6] Y. Li, Q. Wang, E.R. Muir, et al., Retinal vascular and anatomical features in the spontaneously hypertensive rat, Curr. Eye Res. 45 (11) (2020) 1422–1429, https://doi.org/10.1080/02713683.2020.1752738 [published Online First: 20200430].
[7] T. Kida, J. Flammer, H. Oku, et al., Data on the involvement of endothelin-1 (ET-1) in the dysregulation of retinal veins, Data Brief 21 (2018) 59–62, https://doi.org/10.1016/j.dib.2018.09.070 [published Online First: 20180929].
[8] E. Iwasawa, S. Ishibashi, M. Suzuki, et al., Sphingosine-1-Phosphate receptor 1 activation enhances leptomeningeal collateral development and improves outcome after stroke in mice, J. Stroke Cerebrovasc. Dis. 27 (5) (2018) 1237–1251, https://doi.org/10.1016/j.jstrokecerebrovasdis.2017.11.040 [published Online First: 20180111].
[9] M. Ichijo, S. Ishibashi, F. Li, et al., Sphingosine-1-Phosphate receptor-1 selective agonist enhances collateral growth and protects against subsequent stroke, PLoS One 10 (9) (2015) e0138029, https://doi.org/10.1371/journal.pone.0138029 [published Online First: 20150914].
[10] E. Iwasawa, M. Ichijo, S. Ishibashi, et al., Acute development of collateral circulation and therapeutic prospects in ischemic stroke, Neural Regen Res 11 (3) (2016) 368–371, https://doi.org/10.4103/1673-5374.179033.
[11] J.L. Tuttle, B.M. Sanders, H.M. Burkhart, et al., Impaired collateral artery development in spontaneously hypertensive rats, Microcirculation 9 (5) (2002) 343–351, https://doi.org/10.1038/sj.mn.7800151.
[12] I.J. Biose, D. Dewar, I.M. Macrae, et al., Impact of stroke co-morbidities on cortical collateral flow following ischaemic stroke, J Cereb Blood Flow Metab 40 (5) (2020) 978–990, https://doi.org/10.1177/0271678X19858532 [published Online First: 20190624].
[13] D.J. Beard, Z. Li, A.M. Schneider, et al., Rapamycin induces an eNOS (endothelial nitric oxide synthase) dependent increase in brain collateral perfusion in wistar and spontaneously hypertensive rats, Stroke 51 (9) (2020) 2834–2843, https://doi.org/10.1161/STROKEAHA.120.029781 [published Online First: 20200810].
[14] Z. Li, M.J. Cipolla, Mechanisms of flow-mediated dilation of pial collaterals and the effect of hypertension, Hypertension 79 (2) (2022) 457–467, https://doi.org/10.1161/HYPERTENSIONAHA.121.18602 [published Online First: 20211203].
[15] W. Chen, Y. Wu, M. Zheng, et al., Establishing an experimental rat model of photodynamically-induced retinal vein occlusion using erythrosin B, Int. J. Ophthalmol. 7 (2) (2014) 232–238, https://doi.org/10.3980/j.issn.2222-3959.2014.02.08 [published Online First: 2014/04/18].
[16] P. Long, W. Yan, J. Liu, et al., Therapeutic effect of traditional Chinese medicine on a rat model of branch retinal vein occlusion, J Ophthalmol 2019 (2019) 9521379, https://doi.org/10.1155/2019/9521379 [published Online First: 2019/02/18].
[17] T.E. de Carlo, A. Romano, N.K. Waheed, et al., A review of optical coherence tomography angiography (OCTA), Int J Retina Vitreous 1 (2015) 5, https://doi.org/10.1186/s40942-015-0005-8 [published Online First: 20150415].
[18] J.E. Fish, P.A. Marsden, Endothelial nitric oxide synthase: insight into cell-specific gene regulation in the vascular endothelium, Cell. Mol. Life Sci. 63 (2) (2006) 144–162, https://doi.org/10.1007/s00018-005-5421-8.
[19] D. Schuler, R. Sansone, C. Nicolaus, et al., Repetitive remote occlusion (RRO) stimulates eNOS-dependent blood flow and collateral expansion in hindlimb ischemia, Free Radic. Biol. Med. 129 (2018) 520–531, https://doi.org/10.1016/j.freeradbiomed.2018.10.399 [published Online First: 20181015].
[20] U.K. Allahwala, L.M. Khachigian, D. Nour, et al., Recruitment and maturation of the coronary collateral circulation: current understanding and perspectives in arteriogenesis, Microvasc. Res. 132 (2020) 104058, https://doi.org/10.1016/j.mvr.2020.104058 [published Online First: 20200813].
[21] K. Ghimire, J. Zaric, B. Alday-Parejo, et al., MAGI1 mediates eNOS activation and NO production in endothelial cells in response to fluid shear stress, Cells 8 (5) (2019), https://doi.org/10.3390/cells8050388 [published Online First: 20190427].
[22] S.A. Mendoza, J. Fang, D.D. Gutterman, et al., TRPV4-mediated endothelial Ca2+ influx and vasodilation in response to shear stress, Am. J. Physiol. Heart Circ. Physiol. 298 (2) (2010) H466–H476, https://doi.org/10.1152/ajpheart.00854, 2009 [published Online First: 20091204].
[23] L. Xiao, Y. Zhou, T. Friis, et al., S1P-S1PR1 signaling: the "sphinx" in osteoimmunology, Front. Immunol. 10 (2019) 1409, https://doi.org/10.3389/fimmu.2019.01409 [published Online First: 20190625].
[24] E. Jozefczuk, T.J. Guzik, M. Siedlinski, Significance of sphingosine-1-phosphate in cardiovascular physiology and pathology, Pharmacol. Res. 156 (2020) 104793, https://doi.org/10.1016/j.phrs.2020.104793 [published Online First: 20200408].
[25] M. Tölle, L. Klöckl, A. Wiedon, et al., Regulation of endothelial nitric oxide synthase activation in endothelial cells by S1P1 and S1P3, Biochem. Biophys. Res. Commun. 476 (4) (2016) 627–634, https://doi.org/10.1016/j.bbrc.2016.06.009 [published Online First: 20160607].